



# Coverage Probability Enhancement for Better Network Experience of Cell Edge Users in Hierarchical Heterogeneous Networks using Coordinate Aided Transmission Beamforming Model

**E. E Agbon<sup>1\*</sup>, A. S. Yaro<sup>2</sup>, A. D. Usman<sup>3</sup>, M. Umar<sup>4</sup>, A. M. Giwa<sup>5</sup>, A. T. Utev<sup>6</sup>, H. Bello<sup>7</sup>**

<sup>1,2,3,6,7</sup>Department of Electronics and Telecommunication Engineering, Ahmadu Bello University Zaria, Kaduna – Nigeria.

<sup>4</sup>Department of Electrical and Electronics Engineering Technology, Federal Polytechnic Kaura Namoda, – Nigeria.

<sup>5</sup>Department of Information and Communication Engineering, Airforce Institute of Technology Kaduna, – Nigeria.

<sup>1</sup>[eagbonehime1@gmail.com](mailto:eagbonehime1@gmail.com)

Research Article

## Abstract

The problem of interference has led to poor user experience in present day cellular mobile Heterogeneous Network (HetNet). This problem has been compounded in the 5G era due to the massive increase in the number of network users. The shift from voice traffic in the past to data traffic has challenged researchers to develop algorithms to improve the Quality of Service (QoS) of users in the HetNet. The problem of interference has led to poor coverage probability by cell edge users and thus, much focus has been given to cell edge users for better network experience. In an attempt to solve the aforementioned problem, the Separation Architecture (SARC) has been suggested. Here, the control plane and the data plane has been decoupled. The decoupling of these planes has shown better network performance in terms of coverage however, more work needs to be done to improve network users QoS. In the wake of this demand, this research developed a Quality-of-Service Aware control and data plane SARC (QoSA-SARC) algorithm for hierarchical HetNet using a novel Coordinate Aided Transmission (CAT) beamforming model. The QoSA-SARC focuses on improving the probability of coverage provided by the control Base Station (cBS). In the work, simulations were carried out in MATLAB 2017b environment. The results obtained was compared with the work of Liang et al., (2019). Liang et al was used as a basis of comparison because this work considered the same network parameters as that of Liang et al., (2019). Results obtained showed that an improvement of 16.13% and 6.06% at user access rate of  $0.8 \times 10^{-3}$  and  $0.5 \times 10^{-3}$  respectively was achieved when compared with the work of (Liang et al., 2019). Also, the developed algorithm improved the network coverage probability by 10.26% and 8.89% at user service rate  $\mu_c$  of 1/180s and 1/320s respectively.

Copyright © Faculty of Engineering, Ahmadu Bello University, Zaria, Nigeria.

## Keywords

Coordinate Aided Transmission; Coverage Probability; Channel State Information; Interference; Quality of Service; Separation Architecture.

## Article History

Received: January, 2022

Accepted: July, 2022

Reviewed: May, 2022

Published: August, 2022

## 1. Introduction

In the past years, cellular technologies which includes the Third Generation (3G) and Fourth Generation (4G) networks were strictly developed and designed to handle voice services. In the Fifth Generation (5G) era, massive placement of small cells will lead to the development of models that are user-centric. This will be done in order to ensure that user connectivity is uniform and effective. This will in turn improve the quality of user experience (Mustafet al., 2016). Therefore, there will be a great demand of advanced algorithm on both 4G and 5G to meet up to the challenges offered by these technologies. Challenges such as high energy consumption and interference have degraded the smooth operation of the aforementioned technologies (Liu et al., 2016). In a bid to solve the problem of interference, the traditional Heterogeneous Network (H-HetNet) was divided into hierarchy of different tiers. The hierarchical HetNet is so designed to accommodate several technologies which include Device-to-Device, Machine-to-Machine and cellular networks.

Coupling of the control and data plane has been adopted in the traditional cellular network or Conventional Architecture (CARC) for ensuring efficient voice services (Li et al., 2020). The coupling of both the data and the control plane implies that both control and data services will be carried out by a specific base station. The tight coupling of the plane was done to ensure that network users experience efficient coverage and better spectral efficiency during voice-oriented communication (Bhagavatula and Heath, 2011). However, the problem of interference limited the available coverage offered by specific base stations in a network. In an attempt to solve this problem, a lot of algorithms has been introduced by several researcher which include the use of Orthogonal Frequency Division Multiple Access (OFDMA) technology and Radio Resource Management (RRM) techniques. Also, research has proved that the SARC will introduce intra cell interference which will limit the performance of 5G cellular users (Mustafa et al., 2016). Notably, the current interference management techniques only consider the development of algorithms that can mitigate, cancel and coordinate interference without considering the

energy efficiency analysis of the network. (Arora and Jain, 2017).

In a single cell environment, the OFDMA and the RRM techniques has shown promising results in terms of coverage. Furthermore, in a multi-cell scenario, more advanced techniques required to reduce the effect of interference and they include; enhanced ICIC (eICIC), Inter-Cell Interference Coordination (ICIC) and Coordinated Beamforming (CB). The above mentioned techniques are more promising in ensuring better coverage especially for cell edge users. Ensuring better coverage implies that the Quality of Service (QoS) of users will be greatly improved (Mohamed, 2016). The interference management problem has reduced the coverage probability of network users in the control plane. To solve this problem, a QoS aware SARC for H-HetNe was developed (Sugimoto & Jiang, 2011). The separation architecture was developed using coordinated beamforming algorithm. The problem of interference due to the inability of the control plane to share beamformers to data base station users through asymmetric backhaul was solved. The solution was made possible by developing a novel Coordinate Aided Transmission (CAT) model.

A variety of works has been done to improve the quality of service of users using cellular networks in terms of coverage probability. For instance, (Liang *et al.*, 2018) performed an analysis on HetNet relying on control and user plane separation architecture for 5G. The research made use of stochastic geometry to provide an analytical model for cellular radio access networks depending on the advantages of cellular network SARC. The rate requirements of the network users in the control plane and the data plane were separately defined using queuing theory. A downlink transmission in a cellular radio access network that was depending on CD-SARC where cBS and dBS are deployed based on two independent spatial poisson point that is homogeneous was adopted. The control plane and data plane had different channel models where the data plane experienced both Line-of-Sight (LoS) and Non-Line-of-Sight (NLoS) transmission process with the control plane making use of NLoS propagation model. The work analysed the coverage probability for the control plane in order to ensure a reliable coverage. Due to the high data rate requirement of the data plane, the energy efficiency and area spectral efficiency of data plane section of the network was estimated. Numerical result showed that the coverage probability of the control plane can be improved when the density of control Base Stations (cBSs) or service rates are increased. Also, when the dBSs are sparsely deployed, the interference in the network was limited and as such, the Area Spectral Efficiency (ASE) of the data plane increases on time due to the reduction of network path loss and distance of transmission. Despite the commendable result of the research, the analysis did not consider a situation where transmitting BS use beam forming for transmission purposes. And as such, the coverage probability obtained in the analysis was not efficient due to intra-cell interference and this reduced the networks ASE. Also, the research only considered energy efficiency of LoS/NLoS communication with considering the situation where devices can communicate with

each other which is the trending communication technique in 5G. This generally made their obtained energy efficiency model to be inefficient for 5G deployment. Hence, the increase in interference parameter in the network generally would increase the energy consumption rate especially when sent packets experiences failure of transmission. This drawback would make the work to be non-usable in 5G communication. Because, 5G communication requires speed, low energy consumption and high sum rate which cannot be achieved with the current work of the authors.

The energy performance of SARC is a major requirement in ensuring QoS efficient network. Hence, (Zhou *et al.*, 2019) performed an Energy-Spectral Efficiency (ESE) analysis and optimization of HetNet cellular networks. The work also proposed an analytical model for categorizing the achievable ESE of heterogeneous cellular networks, which quantified the relationship that exist amongst the network's ESE and the randomly time-varying large scale user behaviours in conjunction with other network deployment factors. The research specifically modelled the quantitative effect of the cell mobile traffic intensity, the network users' required data rate, the migration factor of the load, and the base station densities on the achievable ESE of network in per-tire-basis, while taking cognisance of the Area-Spectral-Efficiency (ASE) demand. Additionally, a closed-form ESE model was derived, which enabled the researchers to analyse the performance of the network in terms of energy efficiency and spectral efficiency. Also, in order to maximize the ESE of the network under defined outage constraints, an efficient large scale user behaviour aware base station deployment method was developed. The simulation result showed the quantitative and qualitative significance of the energy saving process of the developed algorithm. However, the analytical model developed took into consideration large amount of traffic in a given cell, and this introduced inter-cell interference in the network that resulted in retransmission of traffic in the network. The process of traffic retransmission led to extra energy consumption in the network, which was not captured in the developed model.

In a bid to improve the network sum rate in HetNet (Saini & Kuchi, 2018) made use of Coordinated Multi-Point (CoMP) method to mitigate the effect of interference which translated to better network spectral efficiency. The CoMP additionally made use of channel state information due to the fact that cell edge users experience poor services, the authors optimized the transmit power of these users in order to improve their quality of service. The user allocated at the cell centre were given less attention in terms of power optimization because they have higher probability of enjoying better services. The optimized power led to better network performance at all SNR values. The authors further made use of compression feedback strategy during beamforming which ensured that network resources are optimally utilized for better services. Result from numerous simulations showed that the developed algorithm improved that users network experiences in terms of throughput and feedback efficiency. During the compression process, the use for channel codebook and Eigen mode was used to compress the channel matrix. The recorded drawback of the work was that the network suffered from reduced spectral efficiency and

complexity due to the existence of channel overhead in the network.

(Zhao *et al.*, 2018) performed an Energy-Spectral Efficiency (ESE) analysis and optimization of HetNet cellular networks. The work also proposed an analytical model for categorizing the achievable ESE of heterogeneous cellular networks, which quantified the relationship that exist amongst the network's ESE and the randomly time-varying large scale user behaviours in conjunction with other network deployment factors. The research specifically modelled the quantitative effect of the cell mobile traffic intensity, the network users' required data rate, the migration factor of the load, and the base station densities on the achievable ESE of network in per-tire-basis, while taking cognisance of the Area-Spectral-Efficiency (ASE) demand. Additionally, a closed-form ESE model was derived, which enabled the researchers to analyse the performance of the network in terms of energy efficiency and spectral efficiency. The simulation result showed the quantitative and qualitative significance of the energy saving process of the developed algorithm. However, the analytical model developed took into consideration large amount of traffic in a given cell, and this introduced inter-cell interference in the network that resulted in retransmission of traffic in the network. The process of traffic retransmission led to extra energy consumption in the network, which was not captured in the developed model A control and data plane separation architecture for dual-band mmWave networks was developed by Ansari *et al.*, (2019). In the work, the control base stations were assumed to operate at sub-6GHz single band and the dBS operated at 60GHz licensed band 26GHz unlicensed band. The work formulated a multi-objective optimization problem which was designed to optimize the energy efficiency of the network and the spectral efficiency. To achieve this, a joint radio resource allocation algorithm that was based on lagrangian dual decomposition method was developed. The network model considered in the work was made up of multiple dBS that are within the coverage area of cBS with randomly distributed network users. Furthermore, two cases of CD-SARC were highlighted which included; the case where the cBS serves only the control plane and also the case where the cBS serves both the control plane and the data plane. Results from simulation showed that the developed architecture had an improvement in terms of energy efficiency and spectral efficiency when compared with the traditional maximal-rate and dynamic sub-carriers. However, the communication mode adopted in the work was highly direction. The use of highly directional communication in mmWave band has a short coming in providing an ideal signal coverage that is based on narrow beams. This non deal signal coverage mitigates the performance of dBS as a smaller number of users will be serviced by the BS concerned at a given time. This implies that the sum rate of cell edge users will be inefficient. Since sum rate and energy efficiency are related, the energy efficiency of users in the transmission area will be inefficient.

The main contributions of this paper are summarized as follows. Firstly, the work analyzed the CSI of cellular users. Secondly, the work developed a CAT model to mitigate the level of interference in the network. Lastly, the work developed a model that proofs the relationship between control plane Signal Interference plus Noise Ratio (SINR) and data plane SINR.

## 2. System Models

The system models used in the course of this work are presented.

### 2.1 Beamforming Models

The sharing of beam formers by network base station users with the major aim of ensuring efficient Channel State Information (CSI) in termed coordinated beamforming. Coordinate beamforming is a method used to mitigate the effect of interference in cellular networks. In the wake of 5G, there has been an increasing demand to solve the problem of interference as this mitigates the performance of the network. In this work, a sample three cell model were they all share their CSI is presented as shown in Figure 1. The flowchart for coordinated beamforming in SARC is shown in Figure 2. In SARC, Number of antennas were design to be used by each base station. This number of antennas was so selected to meet up with the high number of users in both the control and data plane.

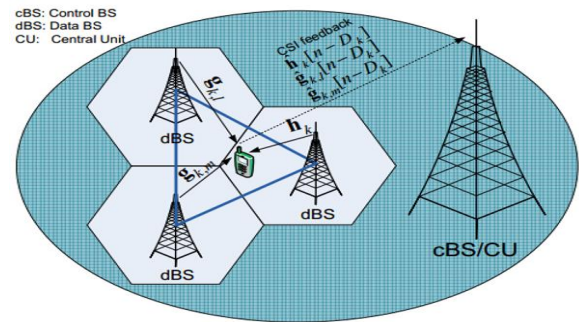


Figure 1: Interference Channels in SARC

The channel that relates to the UE desired channel between  $k^{th}$ BS and  $k^{th}$ UE is given by  $h_k[n] \in \mathbb{C}^{N_t \times 1}$  at  $n^{th}$  defined discrete time. Where  $K^{th}$  BS is the serving BS of  $k^{th}$  user and  $k^{th}$  UE is a specific user equipment in a cell  $g_{k,x}[n]$  is the received CSI of the interfering channel by the BS/dBS,  $h_{k,x}[n]$  is the received CSI of the desired channel by the BS/dBS. By maintaining the same method,  $g_{k,x}[n] \in \mathbb{C}^{N_t \times 1}$  for  $k \neq x$  represents the user interfering channel. In this work, the desired and interfering channels was modelled by using identically distributed Rayleigh fading channel model which has an entry that is a unit variance complex Gaussian function. It can be seen from the Figure 1 that the uplink/downlink desired and interfering channels at the UE are giving as  $h_k$  and  $g_{k,x}$  respectively where  $x \in \{l, m\}$ . The normalization and quantization of the already sent CSI by the control and data plane are respectively given as  $\hat{h}_k[n]$  and  $\hat{g}_{k,x}[n]$ . The process for sending channel direction to the service base station is done in order to ensure limited system feedback. During coordinate beamforming, vectors are selected in such a way that the interfering channel is avoided during data transmission. In the CSI process,  $B_T$  total number of bits are employed for use by data plane user equipment for engaging in feedback process.

During the transmission, the bits for interference and non-interference users ( $B_{k,x}$  and  $B_k$ ) are used in the process of coherently quantizing  $\hat{g}_{k,x}[n]$  and  $\hat{h}_k[n]$  respectively. The process of segregation and forwarding now takes place immediately for better user QoS. This is usually done after all BS has received their CSI information.

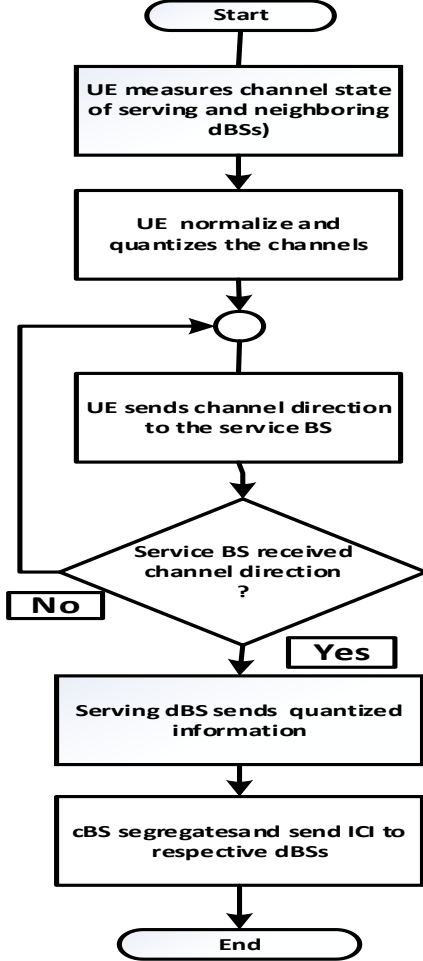


Figure 2: Coordinated Beamforming in SARC (Liang et al., 2019)

## 2.2 System and Channel Models for SARC

The use of stochastic geometry and queuing theory has been a promising candidate for analysing the performance of H-HetNet in terms of coverage probability. In this work, the existence of both NLoS and LoS users in the data plane of SARC was considered. A fading channel model for both data and control plane of SARC was assumed. It is true that the transmission radius of D2D users in the data plane affect the type of transmission sight. Thus, for short ranged transmission, the LoS model is usually adopted for transmission. Since both LoS and NLoS exists in the data plane, the energy efficiency of the data plane is of great importance (Liang et al., 2018). Also, in the system model of SARC, the control plane base station and data plane base station are deployed by the use of

two independent PPP ( $\Psi_c$  and  $\Psi_d$  respectively). The densities of the deployed base stations are respectively  $D_c$  and  $D_d$  (Liang et al., 2018). Additionally, the distribution of control and data plane users is given by  $\Psi_u$  with a corresponding density of network  $D_u$ . The user plane will be made up of D2D devices that will communicate using either D2D communication or cellular communication based on the estimated closeness of centrality. Furthermore, the time interval for each user to access cBS or dBS will be based on exponential distributions with mean value of  $\frac{1}{T_{M_c}}$  (sec) and  $\frac{1}{T_{M_d}}$  (sec) respectively. The arrival rate of the network user's transmission request at the cBS or dBS is given as  $T_{M_c}$  and  $T_{M_d}$  respectively. Also, the holding time for a user that is serviced by cBS or dBS is given by another independent exponential distribution with a mean value of  $\frac{1}{\mu_c}$  (sec) and  $\frac{1}{\mu_d}$  (sec) respectively.

### 2.2.1 Control Plane Traffic Model

Based on Erlang model, the total user traffic load in a given transmission area covered by cBS is given as (Lian et al., 2018):

$$V^c = T_{M_c} N_c \quad (1)$$

$$N_c = \frac{D_u}{D_c} \quad (2)$$

where:  $N_c$  is the average number of users serviced by each cBS. With respect to queuing theory, the queuing model for each cBS is  $M/M/N/N$  and it is associated with an Erlang load of

$$a_c = \frac{v^c}{\mu_c} \quad (3)$$

The probability that  $i$  channels are being used at a given cBS is (Lian et al., 2018):

$$\phi_i^c = \frac{(a_c)^i}{i_{factorial}} \phi_0^c = \frac{(a_c)^i}{i_{factorial}} \left( \sum_{K=0}^N \frac{(a_c)^K}{K_{factorial}} \right)^{-1} \quad (4)$$

where:

$N$  is the number of channels

$k$  denotes any particular channel  $i \in \{1, \dots, N\}$

The probability of a neighbouring cBS interfering with a reference cBS is given as:

$$\rho^c = \sum_{i=1}^N \frac{i}{N} \phi_i^c \quad (5)$$

Hence, the interfering cBS will be distributed based on the poisson point process  $\Psi_I^c$  with density given as (Liang et al., 2018):

$$D_I^c = \rho^c D_c \quad (6)$$

### 2.2.2 Control Plane Channel Model

The downlink channels of cBS show small-scale Rayleigh fading. In this work, we assume that the NLoS transmissions is having a path loss exponent of  $\alpha$  in the control plane. The path gain control plane can be estimated using (Liang et al., 2018):

$$\phi^{cp} = Ar^{-\alpha} \quad (7)$$

where:

$r$  is the transmission distance in the control plane

$A$  is the corresponding path gain at a reference distance of 1 m at the control plane

When considering a user that is relatively close to the cBS, the Signal-to-Interference Noise Ratio (SINR) is given as (Liang *et al.*, 2018):

$$SINR_c = \frac{p_t^c h r^{-\alpha}}{\sum_{k \in \Psi^c} p_t^c h_k r_k^{-\alpha} + \sigma^2} \quad (8)$$

where:

$h$  is the channel gain in the desired link spanning from the  $k_{th}$  cBS interfering cBS

$h_k$  denotes the channel gain in the interfering link spanning from the  $k_{th}$  cBS interfering cBS  $r$  represents the length of the desired link spanning from the  $k_{th}$  cBS interfering cBS

$r_k$  denotes the length of the interfering link spanning from the  $k_{th}$  cBS interfering cBS

$\sigma^2$  is the additive noise

$p_t^c$  represents the cBSs downlink transmission power on each channel

$\Psi$  is the distribution of interfering cBS

Thus, the coverage probability of the control plane which is defined as the probability that a downlink SINR of a user being

above a defined threshold  $\chi_0$  is given as (Liang *et al.*, 2018):

$$\rho^{\text{cov}}(\chi_0, D_c, \alpha) = \Pr[SINR_c > \chi_0] \quad (9)$$

### 2.3 Relationship Between Control Plane and Data Plane SINR

The SINR of the control plane is given as:

$$SINR_c = \frac{p_t^c h r^{-\alpha}}{\sum_{k \in \Psi^c} p_t^c h_k r_k^{-\alpha} + \sigma^2} \quad (10)$$

where:

$h$  is the channel gain in the desired link spanning from the  $k_{th}$  cBS interfering cBS

$h_k$  denotes the channel gain in the interfering link spanning from the  $k_{th}$  cBS interfering cBS

$r$  represents the length of the desired link spanning from the  $k_{th}$  cBS interfering cBS

$r_k$  denotes the length of the interfering link spanning from the  $k_{th}$  cBS interfering cBS

$\sigma^2$  is the additive noise

$p_t^c$  represents the cBSs downlink transmission power on each channel

$\Psi$  is the distribution of interfering cBS

Making the additive noise subject of the formula, we have:

$$\sigma^2 = \frac{p_t^c h r^{-\alpha}}{SINR_c} - \sum_{k \in \Psi^c} p_t^c h_k r_k^{-\alpha} \quad (11)$$

And the SINR of the data plane is given as:

$$SINR_u = \frac{p_t^u A^u h^u r^{-\alpha^u}}{I_T + \sigma^2} \quad (12)$$

where:

$A^u$  is the path loss constant at a reference distance

$\alpha^u$  is the path loss exponent

$H^u$  represents an exponential distribution with unity gain

$I_T$  denotes the cumulative interference power received from all interfering LoS/NLoSdBBS

By making the additive noise subject of the formula, we have:

$$\sigma^2 = \frac{p_t^u A^u h^u r^{-\alpha^u}}{SINR_u} - I_T \quad (13)$$

Comparing Equation (11) and (13), we have the following:

$$\frac{p_t^c h r^{-\alpha}}{SINR_c} - \sum_{k \in \Psi^c} p_t^c h_k r_k^{-\alpha} = \frac{p_t^u A^u h^u r^{-\alpha^u}}{SINR_u} - I_T \quad (14)$$

Note that:

$$I_T = \sum_{k \in \Psi^L} P_t^T A^L h^L r^{-\alpha^L} + \sum_{k \in \Psi^N} P_t^T A^N h^N r^{-\alpha^N} \quad (15)$$

$$EIRP = P_t^T h \quad (16)$$

Further from Equation (14), we have:

$$SINR_c \left( \frac{1}{p_t^c h r^{-\alpha} - SINR_c \sum_{k \in \Psi^c} p_t^c h_k r_k^{-\alpha}} \right) = SINR_u \left( \frac{1}{p_t^u A^u h^u r^{-\alpha^u} - SINR_u I_T} \right) \quad (17)$$

With implementation of the CAT model, the SINR relationship is given as:

$$SINR_c \left( \frac{1}{p_t^c h_{CAT} r^{-\alpha} - SINR_c \sum_{k \in \Psi^c} p_t^c h_{k,CAT} r_k^{-\alpha}} \right) = SINR_u \left( \frac{1}{p_t^u A^u h_{CAT}^u r^{-\alpha^u} - SINR_u I_T} \right) \quad (18)$$

Equation (18) transforms to:

$$I_{T,CAT} = \sum_{k \in \Psi^L} P_t^T A^L h_{CAT}^L r^{-\alpha^L} + \sum_{k \in \Psi^N} P_t^T A^N h_{CAT}^N r^{-\alpha^N} \quad (19)$$

## 3. Methodology

Development of a Coordinate Aided Transmission (CAT) beam forming model for Control and Data plane separation architecture (CD-SARC) the following steps will be carried out:

- i. cBS and dBS are deployed using poisson point process
- ii. Implementing the three-cell network and detached cell to implemented full spectrum re-use
- iii. Assigning dBS to the initialized cells
- iv. All dBS send their location information to neighboring dBSs
- v. All dBSs estimate their coverage area based on reference dBSs.
- vi. Restricting the radiation range of each dBS based on the estimated coverage transmission area
- vii. dBS exchange interfering channel amongst the serving and participating dBSs.
- viii. dBS normalizes and quantizes the channel of participating dBSs
- ix. cBS segregate and forward ICI information to dBSs
- x. CSI/ICI is transmitted back to cBS

The developed architecture for helping the control plane adjust in ensuring coherent beamforming are presented. The sharing of beamformers by the control plane to the data plane will lead to coordinated feedback of CSI which translates to better

coverage probability especially by cell edge users. Figure 3 shows the network cell architecture for improving coverage probability during coordinated beamforming. In the presented model, six network scenarios for ensuring proper coverage is discussed.

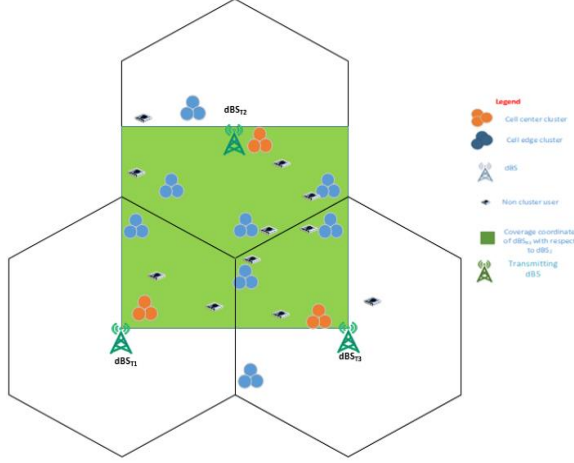


Figure 3: Network Coverage Architecture for CAT Model

The equation representing the total coverage area of the CAT model at a given time is given as:

$$t_{CAT} = [case_1, case_2, case_3, case_4, case_5, case_6] \quad (20)$$

Where the “cases” represents the coverage coordinates for transmission between transmitting dBS and reference dBS. These cases are explained as follows:

#### CASE 1

Therefore, the total coverage coordinates for transmission coordination (see figure 4) between  $dBS_{T1}$  and  $dBS_{R2}$  at points A, B, C and D is given as:

$$t_{CAT-case1} = \left[ (X_o, Y_o), \left( X_o, Y_{\frac{3R}{2}} \right), \left( X_{\frac{\sqrt{3}}{2}R}, Y_{\frac{3R}{2}} \right), \left( X_{\frac{\sqrt{3}}{2}R}, Y_o \right) \right] \quad (21)$$

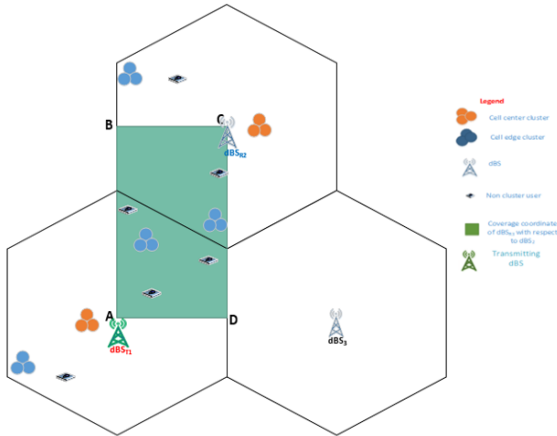


Figure 4: System Model for Estimated Coverage Area of  $dBS_{T1}$  and  $dBS_{R2}$

#### CASE 2

The total coverage coordinates for transmission coordination (see figure 5) between  $dBS_{T1}$  and  $dBS_{R2}$  at points A, E, F and D is given as:

$$t_{CAT-case2} = \left[ (X_o, Y_o), (X_o, Y_R), (X_{R\sqrt{3}}, Y_R), \left( X_{\frac{\sqrt{3}}{2}R}, Y_o \right) \right] \quad (22)$$

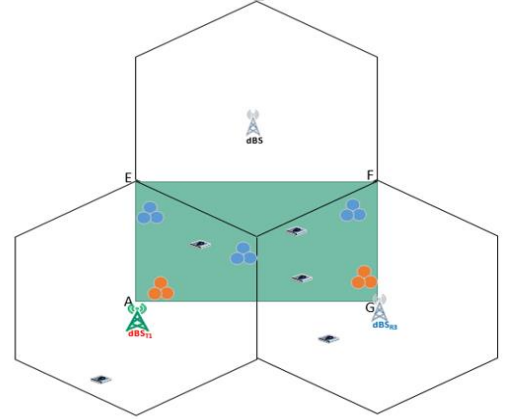


Figure 5: System Model for Estimated Coverage Area of  $dBS_{T1}$  and  $dBS_{R3}$

#### CASE 3

The total coverage coordinates for transmission coordination (see figure 6) between  $dBS_{T2}$  and  $dBS_{R1}$  at points C, B, A and D is given as:

$$t_{CAT-case3} = \left[ (X_o, Y_o), \left( X_o, Y_{\frac{3R}{2}} \right), \left( X_{\frac{\sqrt{3}}{2}R}, Y_{\frac{3R}{2}} \right), \left( X_{\frac{\sqrt{3}}{2}R}, Y_o \right) \right] \quad (23)$$

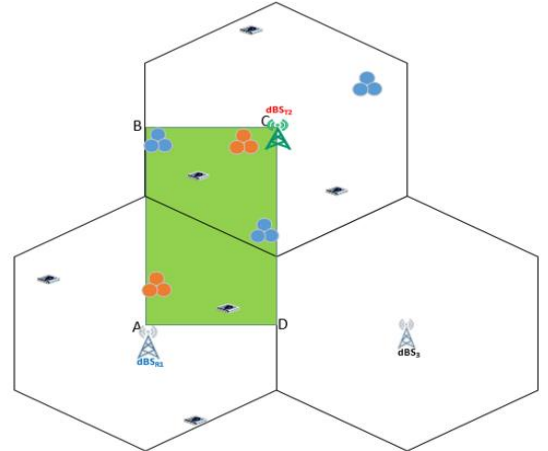


Figure 6: System Model for Estimated Coverage Area of  $dBS_{T2}$  and  $dBS_{R1}$

#### CASE 4

The coordinate points C, B, A, D in case 3 is symmetrical to coordinate points C, D, G and H of case 4. Thus, with respect to the law of symmetry, the  $dBS_{T2}$  coordinates (see figure 7) with respect to  $dBS_{R3}$  for points C, D, G, H is given as:

$$t_{CAT-case4} = \left[ (X_o, Y_o), \left( X_o, Y_{\frac{3R}{2}} \right), \left( X_{\frac{\sqrt{3}}{2}R}, Y_{\frac{3R}{2}} \right), \left( X_{\frac{\sqrt{3}}{2}R}, Y_o \right) \right] \quad (24)$$

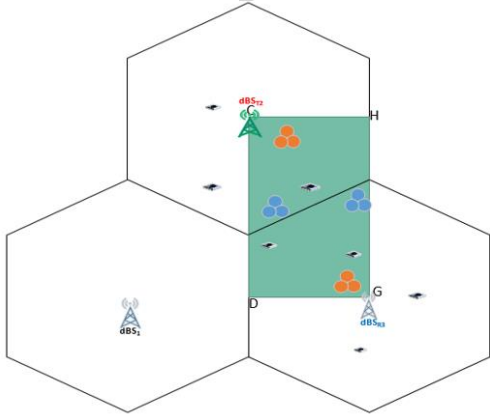


Figure 7: System Model for Estimated Coverage Area of dBS<sub>T2</sub> and dBS<sub>R3</sub>

**CASE 5**

Notice that the coordinate points G, F, E, A in case 5 is symmetrical to coordinate points A, E, F and G of case 2 (see figure 8). Thus, with respect to the law of symmetry, the dBS<sub>T3</sub> coordinates with respect to dBS<sub>R1</sub> for points G, F, E, A is given as:

$$t_{CAT-case5} = \left[ (X_o, Y_o), (X_o, Y_R), (X_{R\sqrt{3}}, Y_R), \left( X_{\frac{\sqrt{3}}{2}R}, Y_o \right) \right] \quad (26)$$

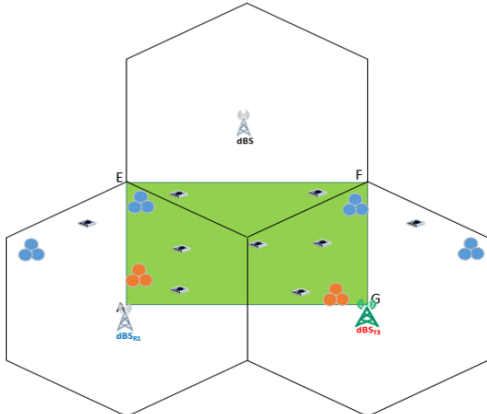


Figure 8: System Model for Estimated Coverage Area of dBS<sub>T3</sub> and dBS<sub>R1</sub>

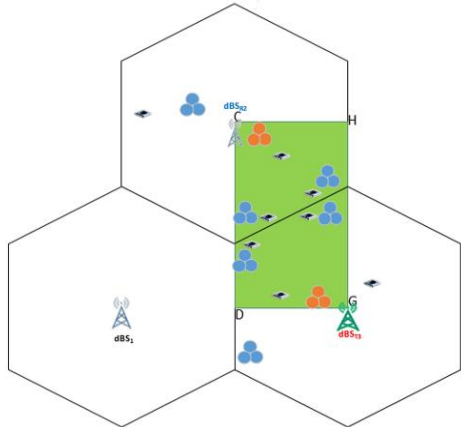


Figure 9: System Model for Estimated Coverage Area of dBS<sub>T3</sub> and dBS<sub>R2</sub>

**CASE 6**

Also, notice that the coordinate points G, H, C, D in case 6 is symmetrical to coordinate points C, D, G and H of case 4 (see Figure 9). Thus, with respect to the law of symmetry, the dBS<sub>T3</sub> coordinates with respect to dBS<sub>R2</sub> for points G, H, C, D is given as:

$$t_{CAT-case6} = \left[ (X_o, Y_o), \left( X_o, Y_{\frac{3R}{2}} \right), \left( X_{\frac{\sqrt{3}}{2}R}, Y_{\frac{3R}{2}} \right), \left( X_{\frac{\sqrt{3}}{2}R}, Y_o \right) \right] \quad (25)$$

It is good to note that the use of the CAT model will help in mitigating interference from other signal sources. The CAT model will help in restricting the radiation region of dBSs and as such, the effective radiated power of dBSs antennas will improve user network experience and will also ensure efficient utilization of dBS transmit power ( $P_t$ ) in a given cell. The simulation parameters are given in Table 1.

Table 1: Simulation Parameters

Parameter	Value
Simulator	MATLAB 2017b
Duplexing, D2D node energy	TDD, 15J
Beamforming	CB
Channel BW	1.4MHz-5.5 GHz
dBS coverage model	CAT model
Latency	10ms
Multi-Antenna Technology	DL: Tx AA, spatial multiplexing, CDD, max 4x4 array
Deployment area of dBS	$0.5 \times 10^{-5}$ to $2 \times 10^{-5}$
Control base station height	30.5 m
Data base station height	12.5m
Data base coverage area	126m-162m
Control plane downlink transmission power on each channel, $P_t^C$	1W
Data plane downlink transmission power on each channel, $P_t^T$	0.4W
Assigned power for BS cooling and mains operation function, $POM$	0.25W
Received desired power from LoS and NLoS dBS, $\sigma^2$	-90dBm
Control plane path gain, $A$	1
LoS path loss constant, $A^L$	$10^{-4.11}$
NLoS path loss constant, $A^N$	$10^{-3.01}$

**4. Simulation Results**

In this section, the coverage probability of the CP was analyzed, which is defined as the probability that the downlink SINR of a user is above a predefined threshold  $\chi_0$ . Ensuring better coverage probability is important as it is a factor for testing the degree of coverage services offered by cBS to especially cell edge users in the control plane.

**4.1 Coverage Probability against SINR Threshold at Varying cBS Users Arrival Rate ( $\lambda_a$ )**

Figures 10 and 11 are plots showing the performance of the work of Liang *et al.*, (2019) and the developed QoS-SA-SARC in terms of control plane coverage probability and SINR threshold at user channel holding time ( $\mu_t$ ) of 1/800s and cBS density ( $\lambda_c$ ) of  $5 \times 10^{-6}$  BSs/m<sup>2</sup> respectively.

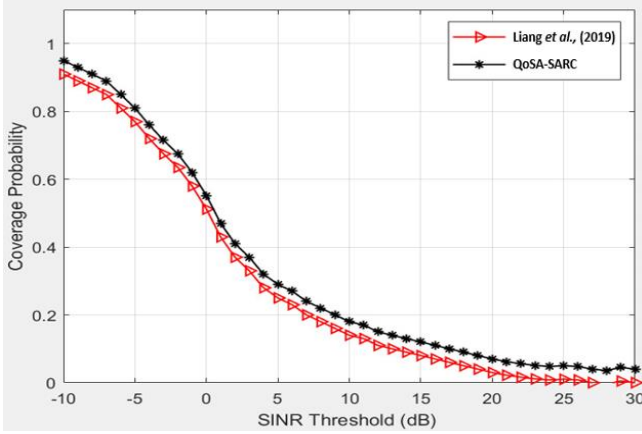


Figure 10: Coverage Probability against SINR Threshold at  $\lambda_a$  of  $0.8 \times 10^{-3}$

It can be observed from the Figure 10 that an increase in the SINR threshold reduces the coverage probability. This is because, increasing the acceptable system standard for SINR will limit the successful coverage offered by serving cBSs to users. The coverage probability in Figure 4.8 was analyzed at  $\lambda_a$  of  $0.8 \times 10^{-3}$ . It can be observed that the QoSA-SARC algorithm has better coverage probability than the existing work. This is due to the efficient service experienced by users due to the use of the CAT model. Hence, network users experience a reduced  $\lambda_a$  and an increase  $\mu_c$ . From the analysis, it can also be observed that the coverage probability increases with decrease in either access rate  $\lambda_a$  or SINR threshold  $\chi_0$ . Also, the coverage probability can be improved by increasing  $\mu_c$  or  $\lambda_c$ . Table 2 shows the percentage improvement of QoSA-SARC over the work Liang et al., (2019). From Figure 10, it can be observed that the QoSA-SARC scheme showed an improvement of 16.13% over the work of Liang et al., (2019) at  $\lambda_a$  having a value of  $0.8 \times 10^{-3}$ . The significance of this result is that users will experience better coverage services.

Table 2: Coverage Probability Improvement at cBS User Arrival Rate ( $\lambda_a$ ) of  $0.8 \times 10^{-3}$

Performance Metric	Liang et al., (2019)	QoSA-SARC	Percentage Improvement
Coverage Probability (Average Value)	0.31	0.36	16.13%

Figure 11 was analyzed at  $\lambda_a$  of  $0.5 \times 10^{-3}$  which shows a slight increase in the coverage probability. This is because, reducing the arrival rate of user request at the cBS will lead to a corresponding decrease in channel interference. Hence, users will experience better coverage. Having better coverage will translate to low rate of dropped packets at the cBS which in turn improves the Quality of Service (QoS) of users. From figure 11, it can be observed that a reduction in  $\mu_c$  and  $\lambda_c$  leads to a corresponding increase in the density of interfering cBSs ( $\lambda_c^f$ ) which results in poor coverage probability. Table 3 shows the percentage improvement of QoSA-SARC over the work Liang et al., (2019). From the figure, it can be observed that a

reduction in  $\mu_c$  and  $\lambda_c$  leads to a corresponding increase in the density of interfering cBSs ( $\lambda_c^f$ ) which results in poor coverage probability. From Figure 10, it can be observed that the QoSA-SARC scheme showed an improvement of 16.13% over the work of Liang et al., (2019) at  $\lambda_a$  having a value of  $0.5 \times 10^{-3}$ . Also, the QoSA-SARC showed an improvement of 6.06% at cBS user arrival rate ( $\lambda_a$ ) of  $0.5 \times 10^{-3}$ .

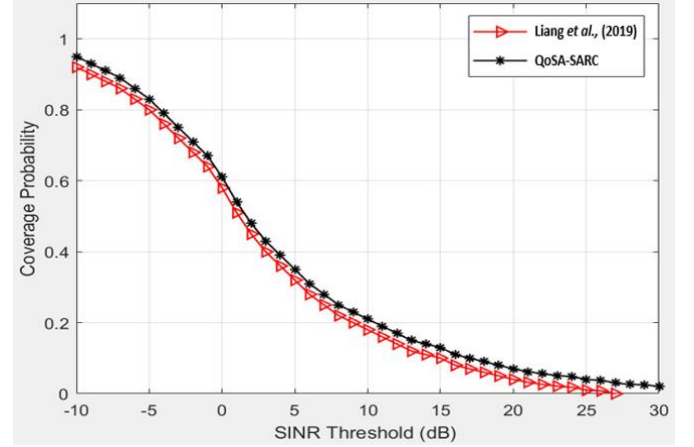


Figure 11: Coverage Probability against SINR Threshold at  $\lambda_a$  of  $0.5 \times 10^{-3}$ .

Table 3: Coverage Probability Improvement at cBS User Arrival Rate ( $\lambda_a$ ) of  $0.5 \times 10^{-3}$

Performance Metric	Liang et al., (2019)	QoSA-SARC	Percentage Improvement
Coverage Probability (Average Value)	0.33	0.35	6.06%

#### 4.2 Coverage Probability against SINR Threshold at Varying cBS Channel Holding Time

Figures 12 and 13 are plots showing the performance of the work of Liang et al., (2019) and the developed QoSA-SARC in terms of control plane coverage probability and SINR threshold at cBS user arrival rates ( $\lambda_a$ ) of  $0.5 \times 10^{-3}$ . Equation (2.29) was used to generate the plots. It can be observed from the figures that increase in the SINR threshold reduces the coverage probability. This is due to the fact that an increase in the network interference will reduce the coverage provided by the cBS especially to cell edge users.

In Figure 12, the coverage probability of the network was analyzed at a cBS user channel holding time ( $\mu_c$ ) of  $\frac{1}{800}$  s and cBS density ( $\lambda_c$ ) of  $6.5 \times 10^{-6}$  BSs/m<sup>2</sup>. It can be observed that an increase in  $\lambda_c$  increases the coverage probability of the network. Also, when the arrival rate of cBS user requests ( $\mu_c$ ) is high, a higher coverage probability can be achieved. From Figure 12, it can be observed that the QoSA-SARC scheme showed an improvement of 10.26% over the work of Liang et al., (2019) at  $\mu_c$  of 1/800s. Table 3 shows the percentage improvement of QoSA-SARC over the work Liang et al., (2019) at  $\mu_c$  of 1/800s.

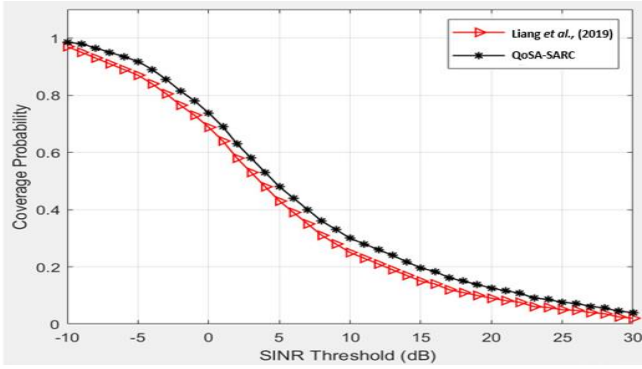


Figure 12: Coverage Probability against SINR Threshold at  $\mu_c$  of  $1/800$ s

Table 4: Coverage Probability Improvement at  $\mu_c$  of  $\frac{1}{800}$  s

Performance Metric	Liang et al., (2019)	QoSA-SARC	Percentage Improvement
Coverage Probability (Average Value)	0.39	0.43	10.26%

In Figure 13, the coverage probability of the network was analyzed at a cBS user channel holding time ( $\mu_c$ ) of  $\frac{1}{320}$  s and cBS density ( $\lambda_c$ ) of  $5 \times 10^{-6}$  BSs/m<sup>2</sup>. It can be observed that an increase in  $\mu_c$  increases the coverage probability of the network. This is because, a user will efficiently use a given channel for transmission purpose if the channel holding time is increased. Thus, better coverage service is experienced by cBS users when  $\mu_c$  is increased. From Figure 13, it can be observed that the QoSA-SARC scheme showed an improvement of 8.89% over the work of Liang et al., (2019) at  $\mu_c$  of  $\frac{1}{320}$  s. This is because, the use of the CAT model at an increased  $\mu_c$  in the control plane will greatly improve the coverage probability due to limited interference.

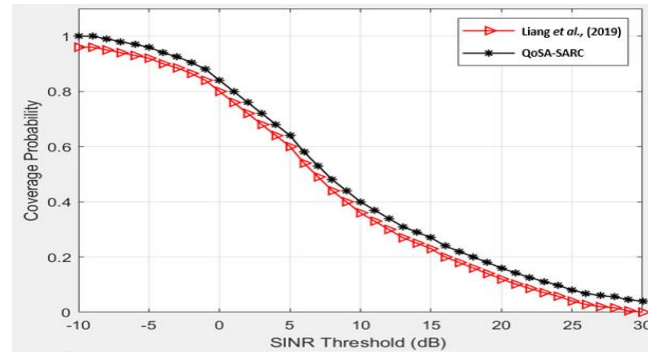


Figure 13: Coverage Probability against SINR Threshold at  $\mu_c$  of  $1/320$ s.

Table 5: Coverage Probability Improvement at  $\mu_c$  of  $\frac{1}{320}$  s

Performance Metric	Liang et al., (2019)	QoSA-SARC	Percentage Improvement
Coverage Probability (Average Value)	0.45	0.49	8.89%

Table 5 shows the percentage improvement of QoSA-SARC over the work Liang et al., (2019). Hence, when the arrival rate

of user requests is high, a higher coverage probability can be achieved by increasing the CBSs’ deployment density or by increasing each CBS’s channel holding time.

## 5. Conclusion

This research has developed a new approach for enhancing the coverage probability hierarchical HetNet using coordinated beamforming. The developed scheme (QoSA-SARC) was able to improve the coverage probability performance of HetNet. The QoSA-SARC made use of CAT model. Also, it’s good to note that as the interfering values goes down with limited CSI, the developed scheme obtained significant coverage probability for low as well high interference parameters. Thus, this showed that cell edge users require will enjoy better service experience.

## References

Ansari, R. I., Pervaiz, H., Chrysostomou, C., Hassan, S. A., Mahmood, A., & Gidlund, M. (2019). Control-Data Separation Architecture for Dual-Band mmWave Networks: A New Dimension to Spectrum Management. *IEEE Access*, 7, 34925-34937.

Arora, M., & Jain, P. C. (2017). Control-and user-plane splitting in small cell architecture of 4G LTE-A”. In *2017 International Conference on Multimedia, Signal, Processing and Communication Technologies (IMPACT)*, 3(5), 75-79.

Bhagavatula R. and Heath R, (2011) Impact of delayed limited feedback on the sum-rate of intercell interference nulling, in Proc. IEEE International Conference on Communications (ICC), 2(5), 1–5.

Li, Y., Xia, M., & Aïssa, S. (2020). Coordinated Multi-Point Transmission: A Poisson-Delaunay Triangulation Based Approach. *IEEE Transactions on Wireless Communications*.

Liu, Q., Wu, G., Guo, Y., Zhang, Y., & Hu, S. (2016, December). Energy efficient resource allocation for control data separated heterogeneous-CRAN. In *2016 IEEE Global Communications Conference (GLOBECOM)* 1(2), 1-6.

Mustafa, H. A. U., Imran, M. A., Shakir, M. Z., Imran, A., & Tafazolli, R. (2016). Separation framework: An enabler for cooperative and D2D communication for future 5G networks. *IEEE Communications Surveys & Tutorials*, 18(1), 419-445.

Mohamed, A. K. A. (2016). *Efficient radio access network with separated control and data functions* (Doctoral dissertation, University of Surrey (United Kingdom). 2(4), 5-9.

Saini, N. K., & Kuchi, K. (2018). *Optimize Power Allocation Scheme to Maximize Sum Rate in CoMP with Limited Channel State Information* (Doctoral dissertation, Indian Institute of Technology Hyderabad).

Sugimoto C. Ni, and J. Jiang (2011), “Degree, Closeness, and Betweenness: Application of group centrality measurements to explore macro-disciplinary evolution diachronically,” in Proc. International Conference of the International Society for Scientometrics&Informetrics (ISSI), 3(3), 1–13.

Zhou, P., Fang, X., Wang, X., & Yan, L. (2019). Multi-Beam Transmission and Dual-Band Cooperation for Control/Data Plane Decoupled WLANs. *IEEE Transactions on Vehicular Technology*. 2(3), 2-15